Bioorganic Chemistry 92 (2019) 103260

Contents lists available at ScienceDirect

Bioorganic Chemistry

journal homepage: www.elsevier.com/locate/bioorg

Novel [1,2,4]triazolo[1,5-*a*]pyrimidine derivatives as potent antitubulin agents: Design, multicomponent synthesis and antiproliferative activities

Fang Yang[a,1], Liang-Zhentian Yu[b,1], Peng-Cheng Diao[a,1], Xie-Er Jian[a], Ming-Feng Zhou[a], Cui-Shan Jiang[a], Wen-Wei You[a], Wei-Feng Ma[b,*], Pei-Liang Zhao[a,*]

[a] Guangdong Provincial Key Laboratory of New Drug Screening, School of Pharmaceutical Science, Southern Medical University, Guangzhou 510515, PR China
[b] Department of Microbiology, School of Public Health and Tropical Medicine, Southern Medical University, Guangzhou 510515, PR China

ARTICLE INFO

Keywords:
Microtubules
[1,2,4]Triazolo[1,5-*a*]pyrimidines
Antiproliferative activity
Tubulin polymerization

ABSTRACT

As restricted CA-4 analogues, a novel series of [1,2,4]triazolo[1,5-*a*]pyrimidines possessing 3,4,5-trimethoxylphenyl groups has been achieved successfully *via* an efficient one-pot three-component reaction of 3-(3,4,5-trimethoxyphenyl)-1H-1,2,4-triazol-5-amine, 1,3-dicarbonyl compounds and aldehydes. Initial biological evaluation demonstrated some of target compounds displayed potent antitumor activity *in vitro* against three cancer cell lines. Among them, the most highly active analogue **26** inhibited the growth of HeLa, and A549 cell lines with IC_{50} values at 0.75, and 1.02 μM, respectively, indicating excellent selectivity over non-tumoural cell line HEK-293 (IC_{50} = 29.94 μM) which suggested that the target compounds might possess a high safety index. Moreover, cell cycle analysis illustrated that the analogue **26** significantly induced HeLa cells arrest in G2/M phase, meanwhile the compound could dramatically affect cell morphology and microtubule networks. In addition, compound **28** exhibited potent anti-tubulin activity with IC_{50} values of 9.90 μM, and molecular docking studies revealed the analogue occupied the colchicine-binding site of tubulin. These observations suggest that [1,2,4]triazolo[1,5-*a*]pyrimidines represent a new class of tubulin polymerization inhibitors and well worth further investigation aiming to generate potential anticancer agents.

1. Introduction

Tubulin is a well-verified therapeutic target for the discovery of highly efficient antitumor drugs due to their crucial roles in cell proliferation, trafficking, signaling and migration in eukaryotic cells [1,2]. To date, tubulin-targeting agents have attracted considerable research interest in anti-cancer therapy [3–5]. Among them, combretastatin A-4 (CA-4, Fig. 1) is the most well-known antitubulin agents, which potently binds to the colchicine binding site leading to significant antiproliferative against multiple human cancer cell lines [6–10], and its water-soluble phosphate prodrug (CA-4P) has been investigated in the ongoing phase II/III clinical trial for the treatment of various cancers, including non-small-cell lung cancer, prostate adenocarcinoma and platinum-resistant ovarian cancer [11–13]. However, the potential clinical applications have so far been halted by the significant toxicities, and *cis-trans* isomerization which results to a sharp reduction in antitumor activity [14]. Recently, fixing *cis*-configuration by replacing the *cis* double-bond with a heterocyclic moiety including fused ring (compounds 3–6, Fig. 1) has proved to be an effective strategy to overcome the isomerization [15–18]. This intrigued us with an ideal to design a series of heterocycle-based conformationally restricted CA-4 analogues.

On the other hand, [1,2,4]triazolo[1,5-*a*]pyrimidines are an important class of bicyclic N-heteroarenes, which have aroused remarkable research attention in very diverse areas ranging from chemotherapy to agriculture due to their diverse biological activities, such as anticancer [19–21], antimicrobial [22], antiviral [23], antibacterial [24], herbicidal [25–28], and fungicidal activities [29]. The diverse bioactivities and the structural similarity with some naturally occurring compounds such as purine make [1,2,4]triazolo[1,5-*a*]pyrimidines promising bicyclic scaffolds to develop new agents for the treatment of different diseases. Inspired by aforementioned findings and following our previous work on the discovery of novel bioactive heterocycles with antitumor potentials [28–33], we herein report a one-pot multicomponent synthesis of a series of new [1,2,4]triazolo[1,5-*a*]pyrimidine derivatives **7**–**30** (Fig. 1) containing a 3,4,5-trimethoxyphenyl fragment as restricted CA-4 analogues, their preliminary antiproliferative and tubulin polymerization inhibitory activities.

* Corresponding authors.
E-mail addresses: maweifeng919@163.com (W.-F. Ma), plzhao@smu.edu.cn (P.-L. Zhao).
[1] These authors contributed equally to this work.

https://doi.org/10.1016/j.bioorg.2019.103260
Received 19 April 2019; Received in revised form 27 August 2019; Accepted 5 September 2019
Available online 10 September 2019

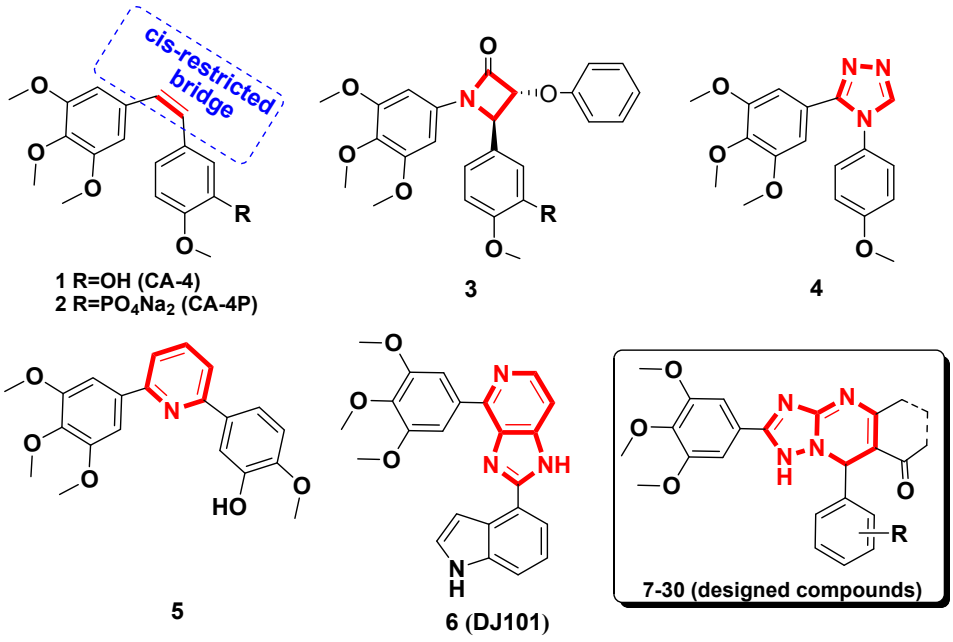

Fig. 1. The structures of CA-4, representative CA-4 analogues with potent anti-tubulin activity and the general structure of target compounds 7–30.

2. Chemistry

The designed [1,2,4]triazolo[1,5-*a*]pyrimidine derivatives **7–30** were prepared in good yields as shown in Scheme 1 *via* a one-pot multicomponent synthesis from 3-(3,4,5-trimethoxyphenyl)-1H-1,2,4-triazol-5-amine, 1,3-dicarbonyl compounds and various aldehydes. To optimize the reaction conditions, a model reaction of 3-(3,4,5-trimethoxyphenyl)-1H-1,2,4-triazol-5-amine (0.3 mmol), cyclohexane-1,3-dione (0.3 mmol) and 4-methylbenzaldehyde (0.3 mmol) was initially investigated in the presence of various catalysts, and solvents under different temperatures. The results are depicted in Table 1 (entries 1–16). It was observed that the efficiency and the yield of the reaction using p-toluenesulfonic acid and DMF at 90 °C (Table 1, entry 6) was higher than those obtained in other catalysts, such as acetic acid, sulfamic acid, hydrochloric acid, and ferric chloride (Table 1, entries 1–5) and other solvents like THF, EtOH, dioxane, DCM and toluene (Table 1, entries 7–10). In addition, amount of catalyst was subsequently examined and it was revealed that a considerable increase or a sharp decrease in amount of catalyst resulted in a reduced yield (Table 1, entries 11–12). Furthermore, we investigated the reaction at different temperatures and reaction times (Table 1, entry 13–16). The procedure in entry 15 was achieved as the best conditions for an efficient one-pot reaction. Having the optimized conditions in hand, we explored the scope of benzaldehydes and 1,3-dicarbonyl compounds (Table 2). All the substrates decorated with electron-withdrawing or

Table 1
Optimization of reaction conditions.[a]

Entry	Catalyst	Mol (%)	solvent	Temperature (°C)	Time (h)	Yield [b] (%)
1	CH_3COOH	5%	DMF	90	10	71
2	NH_2SO_3H	5%	DMF	90	10	49
3	HCl	5%	DMF	90	10	47
4	$FeCl_3$	5%	DMF	90	10	Trace
5	TsOH	5%	DMF	90	10	77
6	TsOH	5%	THF	90	10	75
7	TsOH	5%	Dioxane	90	10	28
8	TsOH	5%	EtOH	90	10	73
9	TsOH	5%	DCM	90	10	60
10	TsOH	5%	Toluene	90	10	54
11	TsOH	10%	DMF	90	10	67
12	TsOH	1%	DMF	90	10	52
13	TsOH	5%	DMF	80	10	30
14	TsOH	5%	DMF	100	10	76
15	TsOH	5%	DMF	90	12	79
16	TsOH	5%	DMF	90	14	78

[a] Reagents and conditions: 3-(3,4,5-trimethoxyphenyl)-1H-1,2,4-triazol-5-amine (0.3 mmol), 4-methyl benzaldehyde (0.3 mmol), cyclohexane-1,3-dione (0.3 mmol), and solvent (5 mL).
[b] Isolated yield.

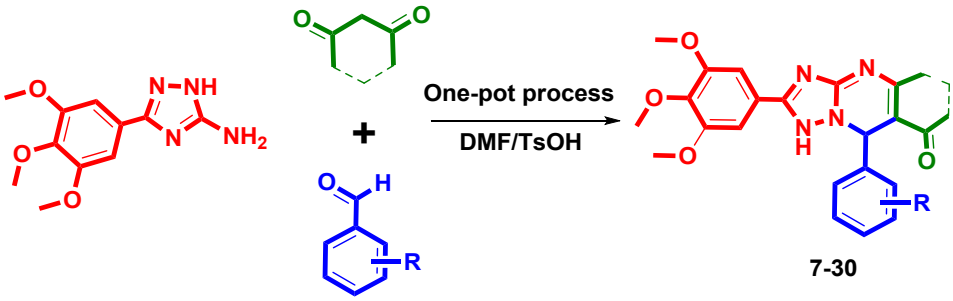

Scheme 1. Synthesis of the target compounds 7–30.

Table 2
Antiproliferative activities of compounds 7–30 against a panel of human cancer cell lines and their cytotoxic effects on the non-tumoural cell line HEK-293.

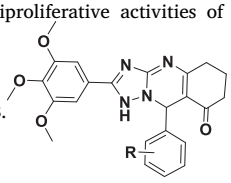

7-24

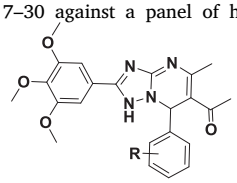

25-30

Comp.	R	IC_{50}(μM)[a]			
		A549	HeLa	HCT116	HEK293[b]
7	4-CH_3	53.14 ± 3.06	62.22 ± 2.19	> 100	NT[c]
8	4-F	92.59 ± 2.80	> 100	98.46 ± 7.48	NT
9	4-NO_2	50.57 ± 2.84	54.87 ± 3.31	86.89 ± 7.77	NT
10	3-F,4-CH_3	94.83 ± 7.47	74.87 ± 4.54	> 100	NT
11	3-F,4-OCH_3	85.64 ± 2.01	63.56 ± 3.75	> 100	NT
12	3,5-Br_2	52.46 ± 7.97	62.36 ± 6.53	97.31 ± 3.45	NT
13	3,4-Cl_2	26.67 ± 0.70	12.20 ± 1.19	28.04 ± 0.66	13.32 ± 2.06
14	2,4-$(OCH_3)_2$	> 100	> 100	> 100	NT
15	4-OCH_3	> 100	59.43 ± 9.33	> 100	> 100
16	3-NO_2,4-OCH_3	94.47 ± 7.57	61.95 ± 3.73	99.04 ± 5.74	NT
17	3,4,5-$(OCH_3)_3$	> 100	72.47 ± 8.54	> 100	NT
18	4-Br	21.33 ± 1.80	36.03 ± 2.85	34.68 ± 1.92	> 100
19	4-CF_3	55.73 ± 4.11	68.92 ± 9.29	93.69 ± 8.16	NT
20	4-CH_2CH_3	65.21 ± 1.04	55.27 ± 2.96	> 100	NT
21	4-CN	95.67 ± 3.80	84.56 ± 0.62	> 100	NT
22	3,4-$(OCH_3)_2$	> 100	79.06 ± 0.89	85.73 ± 7.30	NT
23	3-F	45.82 ± 3.42	17.48 ± 0.74	60.46 ± 9.11	NT
24	3-NO_2	73.93 ± 3.53	78.03 ± 4.18	> 100	NT
25	4-F	5.63 ± 0.28	31.27 ± 0.03	57.33 ± 14.09	> 100
26	4-NO_2	1.02 ± 0.12	0.75 ± 0.02	10.91 ± 0.09	29.94 ± 0.69
27	3-F,4-CH_3	95.86 ± 9.06	> 100	> 100	NT
28	3-NO_2,4-OCH_3	16.08 ± 0.94	9.96 ± 0.05	61.09 ± 10.32	> 100
29	3,5-Br_2	28.28 ± 5.92	37.17 ± 0.64	60.84 ± 1.74	> 100
30	3,4-Cl_2	70.27 ± 3.52	28.67 ± 0.86	> 100	NT
CA-4		0.013 ± 0.006	0.21 ± 0.02	6.10 ± 0.14	NT

[a] 50% inhibitory concentration and mean ± SD of three independent experiments performed in duplicate.
[b] Non-tumoural human embryonic kidney (HEK-293) cell lines.
[c] NT: not tested.

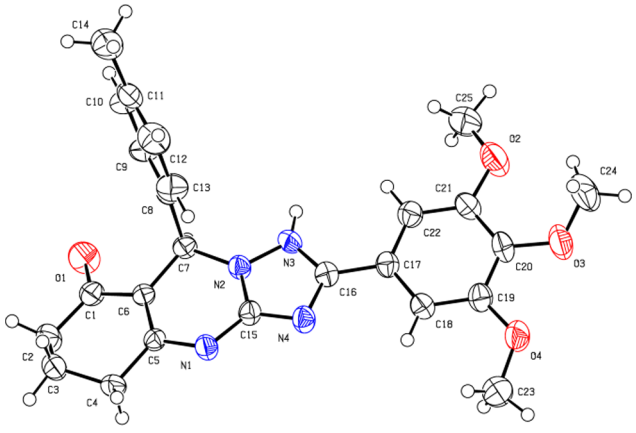

Fig. 2. Molecular structure of compound **7**.

electron-donating groups on the aromatic ring of aryl benzaldehyde smoothly gave a diverse range of [1,2,4]triazolo[1,5-*a*]pyrimidine derivatives **7**–**30** in good yields (53–95%).

The chemical structures of all the synthesized compounds **7**–**30** were characterized with spectroscopic techniques including ^{1}H NMR, ^{13}C NMR, and HRMS, and the spectral data for all the compounds were in full agreement with the proposed structures (see Experimental Section and Supporting Information). The structure of representative compound **7** was confirmed further by single crystal X-ray diffraction. As shown in Fig. 2, the crystal structure showed that the molecular **7** had a characteristic T-shaped conformer, while the planes of the triazole and pyrimidine rings were nearly parallel, with a dihedral angle of 13.29°. In addition, the six-membered cyclohexane ring adopts a chair conformation.

3. Results and discussion

3.1. In vitro antiproliferative activity

Antiproliferative activities of all synthesized [1,2,4]triazolo[1,5-*a*] pyrimidines **7**–**30** *in vitro* was investigated through MTT (3-(4,5-Dimethylthiazol-2-yl)-2,5-diphenyltetrazolium bromide) assay against A549 (human alveolar epithelial cells), HeLa (human cervical cancer cells), and HCT116 (human colon cancer cell lines). The results expressed as the half-maximal inhibitory concentration (IC_{50}) were summarized in Table 2 and one of the most potent anticancer agents, CA-4, was used as a control to compare with the potency of the synthesized [1,2,4]triazolo[1,5-*a*]pyrimidine derivatives. Moreove five selected compounds were evaluated their cytotoxic activity against a representative non-tumoural cell line HEK-293 (human embryonic kidney cells).

For the convenience of structure-activity relationship analysis, compounds **7**–**24** and **25**–**30** were defined as tricyclic and bicyclic triazolopyrimidine derivatives, respectively. As illustrated in Table 2, in general, most of the tested compounds exhibited moderate to strong antiproliferative activities to the A549 and HeLa cell lines, however, for HCT116, most compounds were ineffective (IC_{50} > 100 μM). Noteworthy, the data clearly demonstrated that bicyclic analogues may be

more preferred for increasing the antiproliferative effect than the corresponding tricyclic derivatives, as shown by comparisons between compounds **25** and **8**, **26** and **9**, **28** and **16**, and **29** and **12**. While the most active compound identified in this study was bicyclic analogue **26**, inhibiting the growth of HeLa, A549, and HCT116 cancer cell lines with IC_{50} values at 0.75, 1.02, and 10.91 μM, respectively, which is still remarkably less active than CA-4.

Within the tricyclic triazolopyrimidine series, different antiproliferative activities were observed when various substituents R groups were introduced into the phenyl ring. After the careful analysis of antiproliferative results, it could be observed that analogues (**9**, **12**, **13**, **18**, **23**) bearing electron-withdrawing groups such as 4-nitro, 3,5-dibromo, 3,4-dichloro, 4-bromo, and 3-fluoro on R, exhibited comparatively better inhibition than the corresponding derivatives (**14–17**, **20**, **22**) substituted with electron-donating groups exampled by 2,4-dimethoxy, 4-dimethoxy, 3,4,5-trimethoxy, 4-ethyl, and 3,4-dimethoxy moieties. In bicyclic triazolopyrimidines, of particular note was that this series of compounds exhibited improved potency against tested human cancer lines and excellent selectivity over non-tumoural cell line HEK-293, which indicated that the target compounds might possess a high safety index.

In order to study the mechanism of action of the series of analogues against cancer cells, the highly active compound **26** was selected to evaluate for the effects on the cell cycle progression by flow cytometry. In present work, HeLa cells were treated with 0.75, 1.50 and 3.00 μM concentrations of analogue **26** for 24 h. As depicted in Fig. 3, compound **26** demonstrated 15.03% (0.75 μM), 20.04% (1.50 μM), and 33.47% (3.00 μM) of cell accumulation in G2/M phase, respectively, nevertheless13.72% of G2/M phase for control (untreated cells) was detected. These findings clearly demonstrated that analogue **26** induced a significant G_2/M cell cycle arrest, compared with untreated cells.

To confirm the mechanism of action of these compounds, immunofluorescent assay was carried out to investigate the effect of the most active compound **26** on microtubule networks. As shown in Fig. 4, vehicle treated HeLa cells displayed normal filamentous microtubules arrays. However, the microtubule networks in cytosol were obviously disrupted after treated with **26** at two different concentrations (1.0 and 2.0 μM) for 6 h. These results reveal that **26** acts as an antitubulin

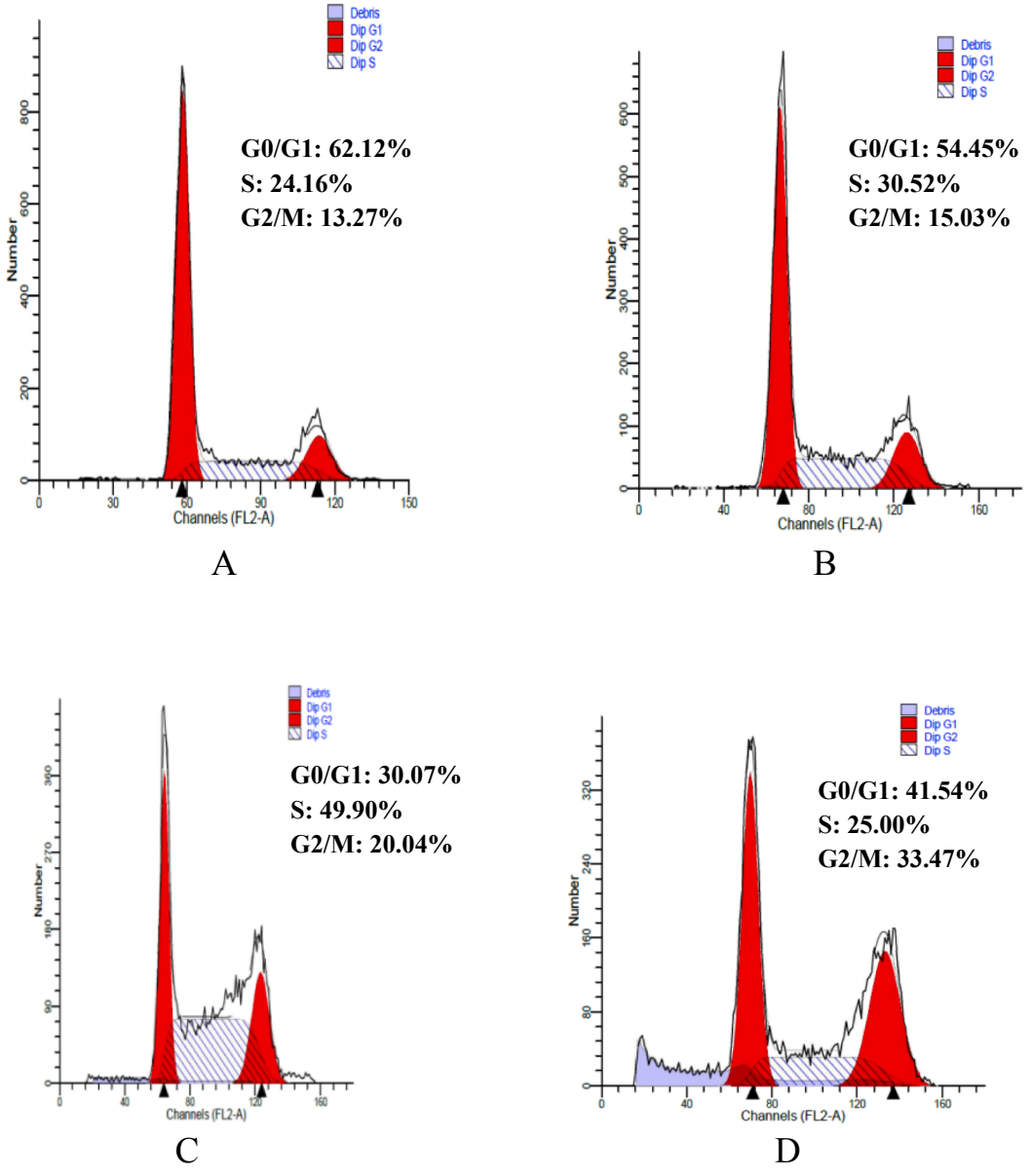

Fig. 3. Effect of compound **26** on cell cycle and apoptosis in HeLa cells. Flow cytometry analysis of HeLa cells treated with **26** for 24 h. (A) Control; (B) **26**, 0.75 μM; (C) **26**, 1.50 μM; (D) **26**, 3.00 μM.

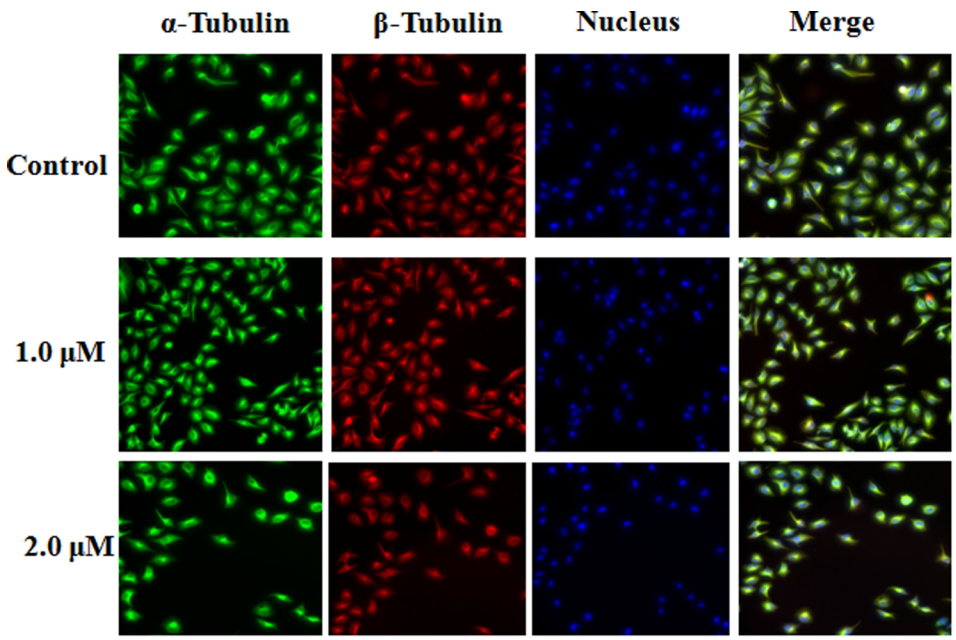

Fig. 4. Effect of compound **26** on tubulin expresion in HeLa cell. Cells were seeded on glass coverslips, incubated with compound **26** (1.0 μM, 2.0 μM) for 6 h, then fixed and processed for confocal microscopy.

inhibitor by inducing a dose-dependent collapse of the microtubule networks.

3.2. Effect of compounds on tubulin polymerization

It has been well reported that tubulin inhibitors preferentially block cell cycle at the G2/M phase [34], so we continued to explore whether microtubule system could be a potential target of these derivatives. Five representative active compounds were then selected for the evaluation of their direct inhibitory effects on tubulin polymerization *in vitro* at 10 μM concentration, and CA-4 was also employed as a positive control. The results were summarized in Table 3. Among them, compound **28** was found to display the best inhibition activity (56%), while CA-4 exhibited a 79% inhibition effect at the tested concentration. Hence, analogue **28** was evaluated for their antitubulin activities relative to that of CA-4 at a 1.5 μM concentration, and the compound inhibited tubulin polymerization in a dose-dependent manner (Fig. 5). Further evaluation manifested that the most potent compound **28** displayed anti-tubulin activity with an IC_{50} value of 9.9 μM, which was in the same range as the reference compound CA-4 (IC_{50} = 4.2 μM).

Because analogue **28**, CA-4, and colchicine possess similar effects on tubulin polymerization, an examination to verify whether these compounds occupy the same binding site on tubulin was carried out. A fluorescence based assay was then performed following previously reported method [35]. And the results (Fig. 6) indicate that **28** competitively inhibits colchicine binding to tubulin and, therefore, that **28** binds to tubulin at the colchicine binding site.

Table 3
Tubulin polymerization inhibitory activities of representative selected compounds.

Comp.	R	Tubulin polymerization	
		% inhibition[a]	IC_{50}(μM)
13	3,4-Cl_2	32	–[b]
16	3-NO_2,4-OCH_3	8	–
25	4-F	33	–
26	4-NO_2	42	–
28	3-NO_2,4-OCH_3	56	9.90
CA-4		79	4.22

[a] Compounds were tested at a final concentration of 10 μM.
[b] –:Not tested.

3.3. Molecular studies

To investigate the possible binding mode for this series of compounds, the most active compound **28** was selected to the molecular docking studies with tubulin crystal structure (PDB: 1SA0). As given in Fig. 7, the 3-nitro, 4-methoxyphenyl ring of the analogue was located deeply into the β-subunit of tubulin. The triazolopyrimidine group and 3,4,5-trimethoxyphenyl ring extend toward the α/β-tubulin interface and derivative **28** forms three important hydrogen bond interactions with amino acids of tubulin. The oxygen of 3-nitro, 4-methoxyphenyl ring established a hydrogen bond with βCys241 (2.6 Å), and one nitrogen atom of triazoloe ring forms a hydrogen bond with βAsn258 (2.7 Å). Furthermore, the residue of αThr178 forms a hydrogen bond with the oxygen of the trimethoxy group (3.3 Å). These molecular docking results further supported the above biological assay data and suggested that analogue **28** may be a potential tubulin inhibitor.

4. Conclusion

In summary, a simple and facile synthesis of a series of novel [1,2,4]triazolo[1,5-*a*]pyrimidines possessing 3,4,5-trimethoxylphenyl groups as restricted CA-4 analogues has been achieved successfully through a one-pot three-component reaction. These new compounds were evaluated for their *in vitro* antiproliferative and tubulin polymerization inhibitory activities. Some of them demonstrated potent antiproliferative activity against employed three human cancer cell lines in this study. Particularly, the most active compound **26** was found to display signifcantly high antiproliferative activity toward HeLa, A549, and HCT116 cell lines with IC_{50} values at 0.75, 1.02, and 10.91 μM, respectively, and to possess the ability to arrest HeLa cells in G2/M phase of the cell cycle. Interestingly, most selected compounds exhibited excellent selectivity over non-tumoural cell line HEK-293, which revealed that these analogues might possess a high safety index. In addition, anti-tubulin investigations displayed that compound **28** exhibited potent anti-tubulin activity. The observations made in this work suggest

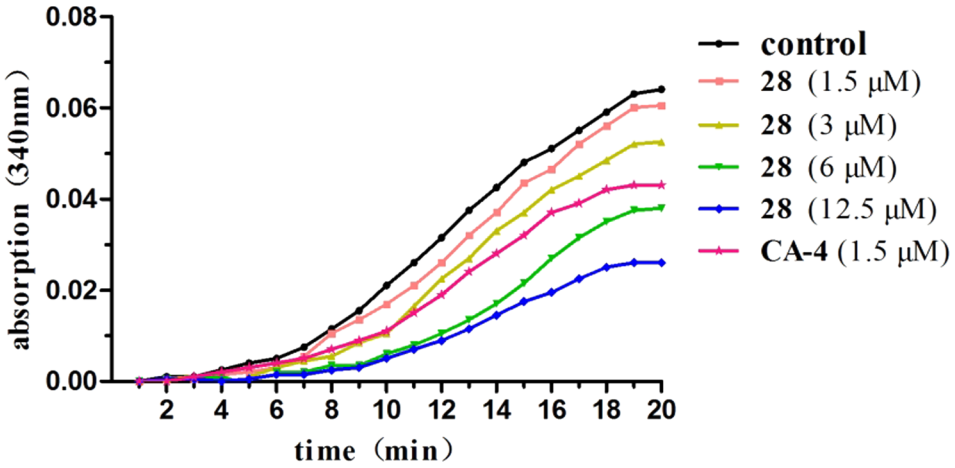

Fig. 5. Effects of **28** on tubulin polymerization *in vitro*. Tubulin in reaction buffer was incubated at 37 °C in the presence of the control (DMSO), compound **28** (1.5, 3.0, 6.0, 12.5 μM) and CA-4 (1.5 μM). The microtubule assembly was measured by spectrophotometry. The experiments were performed three times.

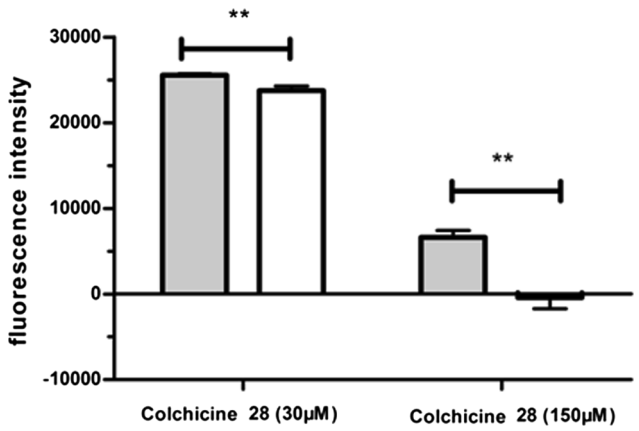

Fig. 6. Plot of fluorescence intensity of formation of the tubulin-colchicine - complex by various concentrations of compound **28**. Tubulin- compound **28** complex was formed by incubating 4 μM tubulin with compound **28** (30 or 150 μM) for 45 min at 37°C. To the solution of this complex was added 4 μM colchicine get tubulin-colchicine complex, and fluorescence spectra were recorded (excitation at 358 nm, emission at 430 nm) after 45 min at 37 °C using a Tecan Spark multimode reader. Spectra comprised of multiple scans from which blank values (buffer alone) were subtracted.

that [1,2,4]triazolo[1,5-*a*]pyrimidines represent a new class of tubulin polymerization inhibitors and may have potential for clinical development as anticancer agents.

5. Experimental protocols

5.1. Chemistry

All reagents and solvents were acquired from commercially available sources and were used without further purification. ^{1}H NMR and ^{13}C NMR spectra were recorded on a Mercury-Plus 400 spectrometer in $CDCl_3$ or DMSO-d_6 solution and chemical shifts (δ) were recorded in parts per million (ppm) with TMS as the internal reference. High-resolution mass spectra (HRMS) carried out on an Agilent QTOF 6540 mass spectrometer. Melting points (mp) were taken on a Buchi B-545 melting point apparatus and are uncorrected.

5.2. General procedure for the preparation of [1,2,4]triazolo[1,5-a] pyrimidine derivatives 7–30

To a mixture of aldehyde (0.3 mmol), cyclohexane-1,3-dione or pentane-2,4-dione (0.3 mmol), 3-(3,4,5-trimethoxyphenyl)-1H-1,2,4-triazol-5-amine (0.3 mmol), p-toluenesulfonic acid (0.015 mmol), and DMF (5 mL) was added. The resulting solution was stirred at 90 °C for 12 h, and was then treated with saturated sodium bicarbonate solution (15 mL) and extracted with EtOAc (3 × 15 mL). The combined organic layers was then dried over anhydrous $MgSO_4$ and evaporated in vacuo. The crude residue was purified by silica gel column chromatography using a mixture of petroleum ether and acetone as an eluent to give the pure solid compounds **7–30** in yields of 53–95%.

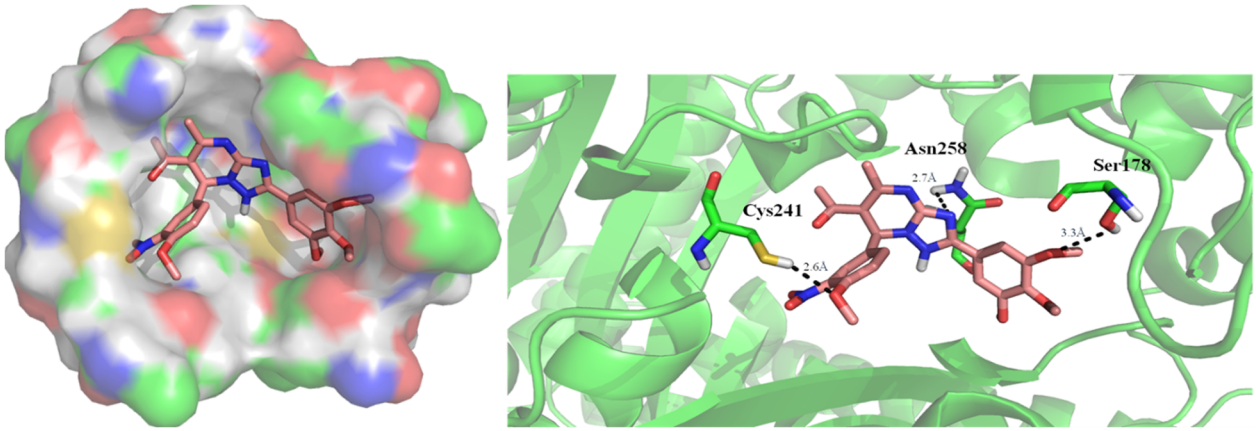

Fig. 7. Proposed binding mode of compound **28** (pink stick) in colchicine binding site of tubulin. The main interacting residues are shown and labeled. The black dashed lines are the potential H-bond between Cys241 (2.6 Å), Ser178 (3.3 Å), Asn258 (2.7 Å). Final figure for docking pose was generated by PyMOL.

5.2.1. p-Tolyl-2-(3,4,5-trimethoxy-phenyl)-5,6,7,9-tetrahydro-1H-[1,2,4] triazolo[5,1-b]quinazolin-8-one (7)

Yield, 79%; mp: 242.2–243.0 °C; ^{1}H NMR (400 MHz, DMSO-d_6) δ: 1.24–1.34 (m, 2H, CH_2), 1.87–2.00 (m, 2H, CH_2), 2 0.23 (s, 3H, CH_3), 2.66 (s, 2H, CH_2), 3.67 (s, 3H, CH_3O), 3.80 (s, 6H, 2 × CH_3O), 6.24 (s, 1H, CH), 7.08–7.14 (m, 4H, ArH), 11.25 (s, 1H, NH). ^{13}C NMR (100 MHz, $CDCl_3$) δ: 193.87, 159.76, 153.33, 149.88, 147.82, 139.34, 137.83, 129.19, 126.88, 125.98, 109.67, 103.76, 60.91, 57.99, 56.21, 36.61, 27.35, 21.10, 20.87. HRMS (ESI) *m/z*: calcd for $C_{25}H_{26}N_4O_4$ (M + H^+) 447.1954 found 447.2025

5.2.2. 9-(4-Fluoro-phenyl)-2-(3,4,5-trimethoxy-phenyl)-5,6,7,9-tetrahydro-1H-[1,2,4]triazolo[5,1-b] quinazolin-8-one (8)

Yield, 77%; mp: 256.1–257.4 °C; ^{1}H NMR (400 MHz, $CDCl_3$) δ: 1.94–2.02 (m, 2H, CH_2), 2.37–2.43 (m, 2H, CH_2), 2.47 (t, J = 5.8 Hz, 2H, CH_2), 3.89 (s, 3H, CH_3O), 3.91 (s, 6H, 2 × CH_3O), 6.52 (s, 1H, CH), 6.99 (t, J = 8.6 Hz, 2H, ArH), 7.22 (s, 2H, ArH), 7.33 (dd, J_1 = 5.6 Hz, J_2 = 8.8 Hz, 2H, ArH), 10.12 (s, 1H, NH). ^{13}C NMR (100 MHz, $CDCl_3$) δ: 193.93, 159.92, 153.38, 150.18, 147.73, 139.48, 136.50, 128.81, 128.73, 125.79, 115.52, 115.30, 109.25, 103.82, 60.92, 57.65, 56.23, 36.57, 27.32, 20.87. HRMS (ESI) *m/z*: calcd for $C_{24}H_{23}FN_4O_4$ (M + H^+) 451.1703 found 451.1769.

5.2.3. 5.1.3 9-(4-Nitro-phenyl)-2-(3,4,5-trimethoxy-phenyl)-5,6,7,9-tetrahydro-1H-[1,2,4]triazolo[5,1-b] quinazolin-8-one (9)

Yield, 91%; mp: 228.5–229.7 °C; ^{1}H NMR (400 MHz, $CDCl_3$) δ: 1.98–2.08 (m, 2H, CH_2), 2.40–2.43 (m, 2H, CH_2), 2.57 (s, 2H, CH_2), 3.89 (s, 3H, CH_3O), 3.91 (s, 6H, 2 × CH_3O), 6.55 (s, 1H, CH), 7.21 (s, 2H, ArH), 7.45 (d, J = 8.0 Hz, 2H, ArH), 7.62 (d, J = 7.6 Hz, 2H, ArH), 9.32 (s, 1H, NH). ^{13}C NMR (100 MHz, $CDCl_3$) δ: 193.77, 160.43, 153.39, 150.42, 147.60, 147.41, 147.19, 139.58, 128.16, 125.51, 123.83, 108.49, 103.69, 60.91, 57.85, 56.24, 36.45, 27.52, 20.79. HRMS (ESI) *m/z*: calcd for $C_{24}H_{23}N_5O_6$ (M − H^+) 476.1648 found 476.1572.

5.2.4. 9-(3-Fluoro-4-methyl-phenyl)-2-(3,4,5-trimethoxy-phenyl)-5,6,7,9-tetrahydro-1H-[1,2,4] triazolo[5,1-b]quinazolin-8-one (10)

Yield, 86%; mp: 255.6–256.4 °C; ^{1}H NMR (400 MHz, $CDCl_3$) δ: 1.92–2.02 (m, 2H, CH_2), 2.23 (s, 3H, CH_3), 2.37–2.42 (m, 2H, CH_2), 2.46 (t, J = 6 Hz, 2H, CH_2), 3.89 (s, 3H, CH_3O), 3.91 (s, 6H, 2 × CH_3O), 6.49 (s, 1H, CH), 6.96 (d, J = 9.2 Hz, 1H, ArH), 7.09 (dd, J_1 = 1.2 HZ, J_2 = 7.6 Hz, 1H, ArH), 7.13 (t, J = 7.6 Hz, 1H, ArH) 7.24 (s, 2H, ArH), 10.19 (s, 1H, NH).^{13}C NMR (100 MHz, $CDCl_3$) δ: 193.86, 159.93, 153.38, 150.16, 147.73, 140.26, 140.20, 139.45, 131.47, 131.42, 125.83, 124.97, 124.80, 122.58, 113.62, 113.39, 109.20, 103.78, 60.92, 57.62, 56.23, 36.57, 27.35, 20.86, 14.25. HRMS (ESI) *m/z*: calcd for $C_{25}H_{25}FN_4O_4$ (M + H^+) 465.1860 found 465.1932.

5.2.5. 9-(3-Fluoro-4-methoxy-phenyl)-2-(3,4,5-trimethoxy-phenyl)-5,6,7,9-tetrahydro-1H-[1,2,4] triazolo[5,1-b]quinazolin-8-one (11)

Yield, 77%; mp: 234.1–235.8 °C; ^{1}H NMR (400 MHz, DMSO-d_6) δ: 1.91–2.02 (m, 2H, CH_2), 2.26–2.31 (m, 2H, CH_2), 2.64–2.68 (m, 2H, CH_2), 3.68 (s, 3H, CH_3O), 3.79 (s, 3H, CH_3O), 3.81 (s, 6H, 2 × CH_3O), 6.25 (s, 1H, CH), 7.01 (d, J = 8.4 Hz, 1H, ArH), 7.07 (d, J = 8 Hz, 1H, ArH), 7.10 (s, 1H, ArH), 7.15 (s, 2H, ArH), 11.27 (s, 1H, NH). ^{13}C NMR (100 MHz, DMSO-d_6) δ: 193.70, 159.52, 153.43, 152.63, 148.03, 138.86, 134.99, 126.55, 123.67, 115.10, 114.04, 107.19, 103.15, 60.50, 57.46, 56.38, 56.21, 36.71, 26.87, 21.05. HRMS (ESI) *m/z*: calcd for $C_{25}H_{25}FN_4O_5$ (M + H^+) 481.1809 found 481.1863.

5.2.6. 9-(3,5-Dibromo-phenyl)-2-(3,4,5-trimethoxy-phenyl)-5,6,7,9-tetrahydro-1H-[1,2,4]triazolo [5,1-b]quinazolin-8-one (12)

Yield, 94%; mp: 261.7–263.6 °C; ^{1}H NMR (400 MHz, DMSO-d_6) δ: 1.90–2.01 (m, 2H, CH_2), 2.25–2.34 (m, 2H, CH_2), 2.62–2.75 (m, 2H, CH_2), 3.69 (s, 3H, CH_3O), 3.81 (s, 6H, 2 × CH_3O), 6.32 (s, 1H, CH), 7.16 (s, 2H, ArH), 7.46 (s, 2H, ArH), 7.73 (s, 1H, ArH), 11.38 (s, 1H, NH). ^{13}C NMR (100 MHz, DMSO-d_6) δ: 193.77, 159.83, 153.47, 148.05, 146.36, 139.02, 133.32, 129.66, 126.33, 122.83, 106.35, 103.27, 60.50, 57.64, 56.24, 36.63, 26.96, 21.00. HRMS (ESI) *m/z*: calcd for $C_{24}H_{22}Br_2N_4O_4$ (M + H^+) 589.0008 found 589.0064.

5.2.7. 9-(3,4-Dichloro-phenyl)-2-(3,4,5-trimethoxy-phenyl)-5,6,7,9-tetrahydro-1H-[1,2,4]triazolo [5,1-b]quinazolin-8-one (13)

Yield, 70%; mp: 261.4–262.6 °C; ^{1}H NMR (400 MHz, $CDCl_3$) δ: 1.94–2.04 (m, 2H, CH_2), 2.38–2.45 (m, 2H, CH_2), 2.50 (s, 2H, CH_2), 3.89 (s, 3H, CH_3O), 3.92 (s, 6H, 2 × CH_3O), 6.45 (s, 1H, CH), 7.22 (s, 2H, ArH), 7.26 (d, J = 8.4 Hz, 1H, ArH), 7.39 (d, J = 1.6 Hz, 1H, ArH), 7.41 (s, 1H, ArH), 10.14 (s, 1H, NH). ^{13}C NMR (100 MHz, $CDCl_3$) δ: 193.87, 160.14, 153.41, 150.51, 147.57, 140.69, 139.58, 132.68, 132.37, 130.49, 128.96, 126.86, 125.58, 108.55, 103.81, 60.93, 57.51, 56.26, 36.50, 27.36, 20.84. HRMS (ESI) *m/z*: calcd for $C_{24}H_{22}Cl_2N_4O_4$ (M − H^+) 499.1018 found 499.1591.

5.2.8. 9-(2,4-Dimethoxy-phenyl)-2-(3,4,5-trimethoxy-phenyl)-5,6,7,9-tetrahydro-1H-[1,2,4]triazolo [5,1-b]quinazolin-8-one (14)

Yield, 65%; mp: 227.1–228.8 °C; ^{1}H NMR (400 MHz, $CDCl_3$) δ: 1.95–2.02 (m, 2H, CH_2), 2.32–2.38 (m, 2H, CH_2), 2.53 (t, J = 5.6 Hz, 2H, CH_2), 3.70 (s, 3H, CH_3O), 3.78 (s, 3H, CH_3O), 3.87 (s, 3H, CH_3O), 3.91 (s, 6H, 2 × CH_3O), 6.40 (s, 1H, CH), 6.49 (d, J = 8.4 Hz, 1H, ArH), 6.54 (s, 1H, ArH), 7.23 (s, 2H, ArH), 7.46 (d, J = 8.4 Hz, 1H, ArH), 9.11 (s, 1H, NH). ^{13}C NMR (100 MHz, $CDCl_3$) δ: 193.93, 160.85, 158.70, 153.24, 139.11, 131.40, 120.75, 108.50, 104.15, 103.58, 99.26, 60.87, 56.31, 56.20, 55.62, 55.23, 36.68, 27.47, 21.01. HRMS (ESI) *m/z*: calcd for $C_{26}H_{28}N_4O_6$ (M − H^+) 491.2009 found 491.1930.

5.2.9. 9-(4-Methoxy-phenyl)-2-(3,4,5-trimethoxy-phenyl)-5,6,7,9-tetrahydro-1H-[1,2,4]triazolo [5,1-b]quinazolin-8-one (15)

Yield, 75%; mp: 248.5–249.4 °C; ^{1}H NMR (400 MHz, DMSO-d_6) δ: 1.89–2.02 (m, 2H, CH_2), 2.25–2.31 (m, 2H, CH_2), 2.67 (d, J = 4 Hz, 2H, CH_2), 3.68 (s, 3H, CH_3O), 3.70 (s, 3H, CH_3O), 3.81 (s, 6H, 2 × CH_3O), 6.24 (s, 1H, CH), 6.85 (d, J = 8.8 Hz, 2H, ArH), 7.15 (s, 2H, ArH), 7.17 (d, J = 8.4 Hz, 2H, ArH), 11.22 (s, 1H, NH). ^{13}C NMR (100 MHz, DMSO-d_6) δ:193.61, 159.38, 159.14, 153.42, 152.23, 148.11, 138.81, 134.41, 128.58, 126.64, 114.09, 107.78, 103.12, 60.49, 57.71, 56.20, 55.46, 36.75, 26.85, 21.09. HRMS (ESI) *m/z*: calcd for $C_{25}H_{26}N_4O_5$ (M − H^+) 461.1903 found 461.1825.

5.2.10. 9-(4-Methoxy-3-nitro-phenyl)-2-(3,4,5-trimethoxy-phenyl)-5,6,7,9-tetrahydro-1H-[1,2,4] triazolo[5,1-b]quinazolin-8-one (16)

Yield, 86%; mp: 233.5–235.0 °C; ^{1}H NMR (400 MHz, DMSO-d_6) δ: 1.92–1.98 (m, 2H, CH_2), 2.23–2.31 (m, 2H, CH_2), 2.69 (s, 2H, CH_2), 3.68 (s, 3H, CH_3O), 3.81 (s, 6H, 2 × CH_3O), 3.88 (s, 3H, CH_3O), 6.35 (s, 1H, CH), 7.15 (s, 2H, ArH), 7.29 (d, J = 8.8 Hz, 1H, ArH), 7.53 (d, J = 8 Hz, 1H, ArH), 7.79 (s, 1H, ArH), 11.35 (s, 1H, NH). ^{13}C NMR (100 MHz, DMSO-d_6)δ: 193.76, 159.70, 153.45, 151.86, 148.01, 139.25, 138.93, 134.51, 133.38, 126.45, 123.86, 114.71, 106.70, 103.20, 60.50, 57.34, 57.11, 56.22, 36.69, 26.93, 21.04. HRMS (ESI) *m/z*: calcd for $C_{25}H_{25}N_5O_7$ (M − H^+) 506.1754 found 506.1670.

5.2.11. 2,9-Bis-(3,4,5-trimethoxy-phenyl)-5,6,7,9-tetrahydro-1H-[1,2,4] triazolo[5,1-b]quinazolin-8- one (17)

Yield, 63%; mp: 275.5–276.5 °C; ^{1}H NMR (400 MHz, $CDCl_3$) δ: 2.03–2.06 (m, 2H, CH_2), 2.40–2.49 (m, 2H, CH_2), 2.53 (t, J_1 = 5.2 Hz, J_2 = 11.6 Hz , 2H, CH_2), 3.82 (s, 3H, CH_3O), 3.84 (s, 6H, 2 × CH_3O), 3.89 (s, 3H, CH_3O), 3.93 (s, 6H, 2 × CH_3O), 6.49 (s, 1H, CH), 6.56 (s, 2H, ArH), 7.26 (s, 2H, ArH), 8.91 (s, 1H, NH). ^{13}C NMR (100 MHz, $CDCl_3$) δ: 193.87, 153.37, 153.23, 149.77, 147.56, 139.44, 138.04, 136.05, 125.92, 109.44, 104.54, 103.74, 60.91, 60.67, 58.16, 56.24, 56.21, 36.61, 29.64, 20.92. HRMS (ESI) *m/z*: calcd for $C_{27}H_{30}N_4O_7$ (M − H^+) 521.2115 found 521.2029.

*5.2.12. 9-(4-Bromo-phenyl)-2-(3,4,5-trimethoxy-phenyl)-5,6,7,9-tetrahydro-1H-[1,2,4]triazolo [5,1-b]quinazolin-8-one (**18**)*

Yield, 87%; mp: 259.5–261.1 °C; ^{1}H NMR (400 MHz, $CDCl_3$) δ: 1.94–2.06 (m, 2H, CH_2), 2.38–2.43 (m, 2H, CH_2), 2.49–2.51 (m, 2H, CH_2), 3.89 (s, 3H, CH_3O), 3.92 (s, 6H, 2 × CH_3O), 6.49 (s, 1H, CH), 7.22 (s, 2H, ArH), 7.23 (d, J = 5.6 Hz, 2H, ArH), 7.44 (d, J = 8 Hz, 2H, ArH), 9.53 (s, 1H, NH). ^{13}C NMR (100 MHz, $CDCl_3$) δ: 193.81, 160.08, 153.38, 149.99, 147.58, 139.61, 131.65, 128.78, 125.76, 122.19, 109.11, 103.75, 60.92, 57.80, 56.24, 36.54, 27.42, 20.84. HRMS (ESI) m/z: calcd for $C_{24}H_{23}BrN_4O_4$ ($M+H^+$) 511.0903 found 511.0968.

*5.2.13. 9-(4-Trifluoromethyl-phenyl)-2-(3,4,5-trimethoxy-phenyl)-5,6,7,9-tetrahydro-1H-[1,2,4] triazolo[5,1-b]quinazolin-8-one (**19**)*

Yield, 77%; mp: 247.3–248.2 °C; ^{1}H NMR (400 MHz, $CDCl_3$) δ: 1.97–2.08 (m, 2H, CH_2), 2.40–2.47 (m, 2H, CH_2), 2.55 (t, J = 5.8 Hz, 2H, CH_2), 3.89 (s, 3H, CH_3O), 3.92 (s, 6H, 2 × CH_3O), 6.58 (s, 1H, CH), 7.22 (s, 2H, ArH), 7.46 (d, J = 8 Hz, 2H, ArH), 7.58 (d, J = 8.4 Hz, 2H, ArH), 9.25 (s, 1H, NH). ^{13}C NMR (100 MHz, $CDCl_3$) δ: 193.80, 160.25, 153.38, 150.19, 147.55, 144.27, 139.50, 127.46, 125.70, 125.56, 125.53, 108.94, 103.70, 99.93, 60.90, 57.90, 56.23, 36.50, 27.47, 20.80. HRMS (ESI) m/z: calcd for $C_{25}H_{23}F_3N_4O_5$ ($M+H^+$) 501.1671 found 501.1740.

*5.2.14. 9-(4-Ethyl-phenyl)-2-(3,4,5-trimethoxy-phenyl)-5,6,7,9-tetrahydro-1H-[1,2,4]triazolo[5,1-b] quinazolin-8-one (**20**)*

Yield, 53%; mp: 248.3–249.8 °C; ^{1}H NMR (400 MHz, $CDCl_3$) δ: 1.21 (t, J = 7.4 Hz, 3H, CH_3), 1.97 (s, 2H, CH_2), 2.32–2.42 (m, 2H, CH_2), 2.45 (s, 2H, CH_2), 2.61 (dd, J_1 = 7.2 Hz, J_2 = 14.4 Hz, 2H, CH_2), 3.89 (s, 3H, CH_3O), 3.90 (s, 6H, 2 × CH_3O), 6.53 (s, 1H, CH), 7.14 (d, J = 8 HZ, 2H, ArH), 7.24 (s, 2H, ArH), 7.28 (d, J = 5.2 HZ, 2H, ArH), 10.05 (s, 1H, NH). ^{13}C NMR (100 MHz, $CDCl_3$) δ: 193.88, 159.77, 153.34, 149.89, 147.87, 139.34, 137.98, 127.99, 126.85, 126.01, 109.72, 103.75, 60.91, 57.93, 56.22, 36.62, 28.44, 27.36, 20.86, 15.23. HRMS (ESI) m/z: calcd for $C_{26}H_{28}N_4O_4$ ($M+H^+$) 461.2111 found 461.2179.

*5.2.15. 4-[8-Oxo-2-(3,4,5-trimethoxy-phenyl)-1,5,6,7,8,9-hexahydro-[1,2,4]triazolo[5,1-b] quinazolin-9-yl]-benzonitrile (**21**)*

Yield, 93%; mp: 245.5–246.8 °C; ^{1}H NMR (400 MHz, $CDCl_3$) δ: 1.99–2.09 (m, 2H, CH_2), 2.42 (t, J = 8 HZ, 2H, CH_2), 2.62 (s, 2H, CH_2), 3.88 (s, 3H, CH_3O), 3.91 (s, 6H, 2 × CH_3O), 6.54 (s, 1H, CH), 7.20 (s, 2H, ArH), 7.44 (d, J = 8 Hz, 2H, ArH), 7.61 (d, J = 8 Hz, 2H, ArH), 9.23 (s, 1H, NH). ^{13}C NMR (100 MHz, $CDCl_3$) δ: 193.78, 160.37, 153.40, 150.44, 147.52, 145.39, 139.58, 132.39, 127.93, 125.58, 118.45, 112.03, 108.52, 103.71, 60.91, 58.02, 56.24, 36.47, 27.48, 20.79. HRMS (ESI) m/z: calcd for $C_{25}H_{23}N_5O_4$ ($M+H^+$) 458.1750 found 458.1814.

*5.2.16. 9-(3,4-Dimethoxy-phenyl)-2-(3,4,5-trimethoxy-phenyl)-4a,5,6,7,8a,9-hexahydro-1H-[1,2,4] triazolo[5,1-b]quinazolin-8-one (**22**)*

Yield, 62%; mp: 234.1–235.8 °C; ^{1}H NMR (400 MHz, $CDCl_3$) δ: 1.95–2.05 (m, 2H, CH_2), 2.34–2.38 (m, 2H, CH_2), 2.52 (d, J = 5.6 Hz, 2H, CH_2), 3.70 (s,3H, CH_3O), 3.78 (s, 3H, CH_3O), 3.87 (s, 3H, CH_3O), 3.91 (s, 6H, 2 × CH_3O), 6.40 (s, 1H, CH), 6.49 (d, J = 8.4 Hz, 1H, ArH), 6.54 (s, 1H, ArH), 7.23 (s, 1H, ArH), 7.46 (d, J = 8.4 Hz, 1H, CH), 9.11 (s, 1H, NH). ^{13}C NMR (100 MHz, DMSO-d_6) δ: 193.36, 160.68, 158.94, 158.73, 153.39, 152.58, 148.53, 138.66, 131.09, 126.87, 122.21, 106.69, 105.09, 103.02, 99.64, 60.48, 56.26, 56.17, 55.56, 36.87, 26.88, 21.20. HRMS (ESI) m/z: calcd for $C_{26}H_{28}N_4O_6$ ($M-H^+$) 491.2009 found 491.1928.

*5.2.17. 9-(3-Fluoro-phenyl)-2-(3,4,5-trimethoxy-phenyl)-5,6,7,9-tetrahydro-1H-[1,2,4]triazolo [5,1-b]quinazolin-8-one (**23**)*

Yield, 85%; mp: 248.9–249.6 °C; ^{1}H NMR (400 MHz, DMSO-d_6) δ: 1.91–2.02 (m, 2H, CH_2), 2.28–2.32 (m, 2H, CH_2), 2.62–2.74 (m, 2H, CH_2), 3.68 (s, 3H, CH_3O), 3.81 (s, 6H, 2 × CH_3O), 6.32 (s, 1H, CH), 7.09 (t, J = 8 Hz, 3H, ArH), 7.16 (s, 2H, ArH), 7.35 (dd, J_1 = 7.6 Hz, J_2 = 14.4 Hz, 1H, ArH), 11.32 (s, 1H, NH). ^{13}C NMR (100 MHz, DMSO-d_6) δ: 193.70, 163.62, 161.20, 159.64, 153.45, 152.88, 148.11, 144.71, 138.94, 130.84, 130.75, 126.48, 123.48, 115.14, 114.93, 114.50, 114.29, 107.02, 103.22, 60.50, 57.83, 56.22, 36.68, 26.88, 21.01. HRMS (ESI) m/z: calcd for $C_{24}H_{23}FN_4O_4$ ($M+H^+$) 451.1703 found 451.1769.

*5.2.18. 9-(3-Nitro-phenyl)-2-(3,4,5-trimethoxy-phenyl)-5,6,7,9-tetrahydro-1H-[1,2,4]triazolo[5,1-b] quinazolin-8-one (**24**)*

Yield, 93%; mp: 249.9–250.5 °C; ^{1}H NMR (400 MHz, DMSO-d_6) δ: 1.91–1.99 (m, 2H, CH_2), 2.23–2.32 (m, 2H, CH_2), 2.70 (s, 2H, CH_2), 3.68 (s, 3H, CH_3O), 3.80 (s, 6H, 2 × CH_3O), 6.49 (s, 1H, CH), 7.15 (s, 2H, ArH), 7.63 (d, J = 7.2 Hz, 1H, ArH), 7.71 (d, J = 7.2 Hz, 1H, ArH), 8.12 (d, J = 7.2 Hz, 2H, ArH), 11.44 (s, 1H, NH). ^{13}C NMR (100 MHz, DMSO-d_6) δ: 193.78, 159.85, 153.45, 153.20, 148.12, 144.01, 138.97, 134.13, 130.52, 126.35, 123.26, 122.23, 106.65, 103.21, 60.49, 57.87, 56.21, 36.63, 26.93, 21.02. HRMS (ESI) m/z: calcd for $C_{24}H_{23}N_5O_6$ ($M+H^+$) 478.1648 found 478.1720.

*5.2.19. 1-[7-(4-Fluoro-phenyl)-5-methyl-2-(3,4,5-trimethoxy-phenyl)-1,7-dihydro-[1,2,4]triazolo [1,5-a]pyrimidin-6-yl]-ethanone (**25**)*

Yield, 82%; mp: 232.8–233.4 °C; ^{1}H NMR (400 MHz, $CDCl_3$) δ: 2.20 (s, 3H, CH_3), 2.42 (s, 3H, CH_3), 3.89 (s, 3H, CH_3O), 3.93 (s, 6H, 2 × CH_3O), 6.55 (s, 1H, CH), 7.04 (t, J = 8.6 Hz, 2H, ArH), 7.22 (s, 2H, ArH), 7.40–7.43 (m, 2H, ArH), 8.75 (s, 1H, NH). ^{13}C NMR (100 MHz, $CDCl_3$) δ: 195.21, 160.26, 153.31, 146.94, 143.96, 139.30, 135.98, 129.32, 129.24, 125.92, 115.91, 115.69, 108.91, 103.44, 60.88, 59.67, 56.16, 30.29, 20.73. HRMS (ESI) m/z: calcd for $C_{23}H_{23}FN_4O_4$ ($M+H^+$) 439.1703 found 439.1773.

*5.2.20. 1-[5-Methyl-7-(4-nitro-phenyl)-2-(3,4,5-trimethoxy-phenyl)-1,7-dihydro-[1,2,4]triazolo [1,5-a]pyrimidin-6-yl]-ethanone (**26**)*

Yield, 92%; mp: 249.5–251.2 °C; ^{1}H NMR (400 MHz, $CDCl_3$) δ: 2.29 (s, 3H, CH_3), 2.52 (s, 3H, CH_3), 3.89 (s, 3H, CH_3O), 3.92 (s, 6H, 2 × CH_3O), 6.65 (s, 1H, CH), 7.21 (s, 2H, ArH), 7.58 (d, J = 8.4 Hz, 2H, ArH), 8.21 (d, J = 8.4 Hz, 2H, ArH), 8.31 (s, 1H, NH). ^{13}C NMR (100 MHz, $CDCl_3$) δ: 194.32, 160.59, 153.35, 147.78, 147.24, 147.14, 144.61, 128.37, 124.01, 109.38, 103.53, 99.92, 60.89, 59.46, 56.18, 30.98, 20.93. HRMS (ESI) m/z: calcd for $C_{23}H_{23}N_5O_6$ ($M-H^+$) 464.1648 found 464.1575.

*5.2.21. 1-[7-(3-Fluoro-4-methyl-phenyl)-5-methyl-2-(3,4,5-trimethoxy-phenyl)-1,7-dihydro-[1,2,4] triazolo[1,5-a]pyrimidin-6-yl]-ethanone (**27**)*

Yield, 88%; mp: 223.0–225.3 °C; ^{1}H NMR (400 MHz, $CDCl_3$) δ: 2.21 (s, 3H, CH_3), 2.25 (s, 3H, CH_3), 2.47 (s, 3H, CH_3), 3.89 (s, 3H, CH_3O), 3.93 (s, 6H, 2 × CH_3O), 6.50 (s, 1H, CH), 7.06 (d, J = 10.0 Hz, 1H, ArH), 7.14 (dd, J_1 = 7.6 Hz, J_2 = 12.8 Hz, 2H, ArH), 7.23 (s, 2H, ArH), 8.25 (s, 1H, NH). ^{13}C NMR (100 MHz, $CDCl_3$) δ: 195.15, 160.24, 153.31, 146.97, 144.13, 139.70, 139.64, 139.26, 131.78, 125.92, 122.84, 114.19, 113.95, 108.69, 103.40, 60.88, 59.71, 56.15, 30.28, 20.77, 14.26. HRMS (ESI) m/z: calcd for $C_{24}H_{25}FN_4O_4$ ($M+H^+$) 453.1860 found 453.1926.

*5.2.22. 1-[7-(4-Methoxy-3-nitro-phenyl)-5-methyl-2-(3,4,5-trimethoxy-phenyl)-1,7-dihydro-[1,2,4] triazolo[1,5-a]pyrimidin-6-yl]-ethanone (**28**)*

Yield, 89%; mp: 249.5–251.2 °C; ^{1}H NMR (400 MHz, DMSO-d_6) δ: 2.22 (s, 3H, CH_3), 2.47 (s, 3H, CH_3), 3.69 (s, 3H, CH_3O), 3.80 (s, 6H, 2 × CH_3O), 3.89 (s, 3H, CH_3O), 6.56 (s, 1H, CH), 7.17 (s, 2H, ArH), 7.33 (d, J = 8.8 Hz, 1H, ArH), 7.60 (dd, J_1 = 2.4 Hz, J_2 = 8.8 Hz, 1H, ArH), 7.83 (d, J = 2 Hz, 1H, ArH), 11.03 (s, 1H, NH). ^{13}C NMR (100 MHz, DMSO-d_6) δ: 194.75, 159.83, 153.44, 152.06, 148.02, 139.32, 138.90, 134.65, 133.54, 126.50, 123.86, 115.05, 108.12, 103.17, 60.50, 58.60, 57.14, 56.20, 31.23, 20.22. HRMS (ESI) m/z: calcd for $C_{22}H_{24}N_5O_7$ ($M-H^+$) 494.1754 found 494.1766.

*5.2.23. 1-[7-(3,5-Dibromo-phenyl)-5-methyl-2-(3,4,5-trimethoxy-phenyl)-1,7-dihydro-[1,2,4]triazolo [1,5-a]pyrimidin-6-yl]-ethanone (**29**)*

Yield, 95%; mp: 241.3–242.5 °C; ^{1}H NMR (400 MHz, DMSO-d_6) δ: 2.25 (s, 3H, CH_3), 2.49 (s, 3H, CH_3), 3.69 (s, 3H, CH_3O), 3.81 (s, 6H, 2 × CH_3O), 6.49 (s, 1H, CH), 7.16 (s, 2H, ArH), 7.50 (s, 2H, ArH), 7.76 (s, 1H, ArH), 11.07 (s, 1H, NH). ^{13}C NMR (100 MHz, DMSO-d_6) δ: 194.61, 159.97, 153.46, 148.02, 147.29, 146.60, 138.97, 133.56, 129.61, 126.36, 123.06, 108.12, 103.23, 60.50, 58.86, 56.21, 31.43, 20.31. HRMS (ESI) *m/z*: calcd for $C_{23}H_{22}Br_2N_4O_4$ ($M+H^+$) 577.0008 found 577.0063.

*5.2.24. 1-[7-(3,4-Dichloro-phenyl)-5-methyl-2-(3,4,5-trimethoxy-phenyl)-1,7-dihydro-[1,2,4]triazolo [1,5-a]pyrimidin-6-yl]-ethanone (**30**)*

Yield, 73%; mp: 233–236.4 °C; ^{1}H NMR (400 MHz, DMSO-d_6) δ: 2.23 (s, 3H, CH_3), 2.47 (s, 3H, CH_3), 3.68 (s, 3H, CH_3O), 3.80 (s, 6H, 2 × CH_3O), 6.52 (s, 1H, CH), 7.14 (s, 2H, ArH), 7.28 (dd, J_1 = 2.0 Hz, J_2 = 8.4 Hz, 1H, ArH), 7.61 (d, J_1 = 8.4 Hz, 2H, ArH), 11.07 (s, 1H, NH). ^{13}C NMR (100 MHz, $CDCl_3$) δ: 194.52, 160.28, 153.37, 147.39, 144.82, 140.51, 139.42, 132.99, 132.83, 130.75, 129.18, 126.99, 125.55, 108.95, 103.55, 60.95, 59.24, 56.18, 30.84, 20.79. HRMS (ESI) *m/z*: calcd for $C_{23}H_{22}Cl_2N_4O_4$ ($M-H^+$) 487.1018 found 487.0931.

5.3. Biological evaluation

5.3.1. Antiproliferative activity

The anticancer potency of analogues **7–30** were evaluated *in vitro* against a panel of three different human cancer cell lines, A549, HeLa, and HCT116 by the standard MTT (3-(4,5-dimethylthiazol-2-yl)-2,5-diphenyltetrazolium bromide) assay. The above cell lines were cultured in RPMI-1640 medium supplemented with 10% FBS. Determined compounds were dissolved in dimethyl sulfoxide (DMSO) at 100 mM and diluted into a series of concentrations with the medium. Exponentially growing cells were plated in 96-well plates (2×10^3 cells/well) and incubated for 48 h at 37 °C for attachment. The culture medium was then changed, and cells grew in medium with the tested compounds. DMSO (0.1%) and CA-4 were used as negative and positive control, respectively. Cells were incubated at 37 °C for 48 h. After the treatment period, 10 μL of MTT solution (5 mg/mL) was added to each well, and the plates were incubated for 4 h at 37 °C. The medium was then aspirated and formazan crystals were dissolved in DMSO (150 μL) for about 10 mins. The absorbance at 570 nm (Abs) of the suspension was measured by a microplate reader (Bio-Rad laboratories, USA). The inhibition percentage was obtained by using the following formula: % inhibition = ($Abs_{control}$-$Abs_{compound}$)/$Abs_{control}$ × 100%. IC_{50} values of the tested compounds and CA-4 were amounted through treating cells with drugs of various concentrations and calculated using the prism statistical package (GraphPad Software, San Diego, CA, U.S.A.).

5.3.2. Flow-activating cell sorting (FACS) analysis

The effect of analogue **26** on cell cycle phase distribution of human cervical cancer cell lines (HeLa) was investigated by the flow cytometric analysis. When the cells grew to about 70–80% confluence in 60 mm dishes over night, they were incubated with compound **26** at 0.75, 1.50, and 3.00 μM concentrations for 24 h. Subsequently, control and treated cells were harvested, washed with PBS, and fixed in 75% ice-cold ethanol at 4 °C overnight. They were then washed with PBS, incubated with 50 μg/mL of RNase for 30 min at 37 °C, stained with 50 μg/mL of propidium iodide, and subjected to flow cytometry (Beckman Coulter).

5.3.3. Immunofluorenscence assay

Immunofluorenscence assay studies were performed following our previously reported method [30].

5.3.4. In vitro tubulin polymerization assay

The tubulin polymerization activity *in vitro* was carried out according to our previously described method [33].

5.3.5. Molecular modeling

Molecular docking studies were performed using the Surflex module of Sybyl 7.3 package [36], and the tubulin structure (code: 1SA0) was obtained from the PDB data bank (http://www.rcsb.org/-PDB) [37]. The studied molecule was initially prepared in Sybyl 7.3, and energy minimization was carried out by using the Tripos force field with a distance–dependent dielectric and powell gradient algorithm with a convergence criterion of 0.001 kcal/mol Å. In addition, partial atomic charges were analyzed using Gasteiger–Hückel method, and all the other parameters were assigned default values throughout the docking process. The top 20 conformations with different scores were acquired, and the best ranking pose was visualized with Pymol [38].

Acknowledgements

The present research was supported by the National Natural Science Foundation of China (21372113), the Science and Technology Program of Guangzhou, China (201707010198), and the Natural Science Foundation of Guangdong Province, China (2018B030311067).

Appendix A. Supplementary material

Supplementary data to this article can be found online at https://doi.org/10.1016/j.bioorg.2019.103260.

References

[1] C. Dumontet, M.A. Jordan, Microtubule-binding agents: a dynamic field of cancer therapeutics, Nat. Rev. Drug Discov. 9 (2010) 790–803.
[2] H. Kadavath, R.V. Hofele, J. Biernat, S. Kumar, K. Tepper, H. Urlaub, E. Mandelkow, M. Zweckstetter, Tau stabilizes microtubules by binding at the interface between tubulin heterodimers, Proc. Natl. Acad. Sci. USA 112 (2015) 7501–7506.
[3] G.J. Brouhard, L.M. Rice, Microtubule dynamics: an interplay of biochemistry and mechanics, Nat. Rev. Mol. Cell Biol. 19 (2018) 451–463.
[4] Y. Zhang, H. Yang, J. Liu, Q. Deng, P. He, Y. Lin, J. Jiang, X. Gu, M. Mo, H. Pan, X. Xiong, Y. Qiu, J. He, High expression levels of class III β-tubulin in resected non-small cell lung cancer patients are predictive of improved patient survival after vinorelbine-based adjuvant chemotherapy, Oncol Lett. 6 (2013) 220–226.
[5] J. Zhou, S. Qian, H. Li, W. He, X. Tan, Q. Zhang, G. Han, G. Chen, R. Luo, Predictive value of microtubule-associated protein Tau in patients with recurrent and metastaticbreast cancer treated with taxane-containing palliative chemotherapy, Tumour Biol. 36 (2015) 3941–3947.
[6] D. Lamaa, H.P. Lin, L. Zig, C. Bauvais, G. Bollot, J. Bignon, H. Levaique, O. Pamlard, J. Dubois, M. Ouaissi, M. Souce, A. Kasselouri, F. Saller, D. Borgel, C. Jayat-Vignoles, H. Al-Mouhammad, J. Feuillard, K. Benihoud, M. Alami, A. Hamze, Design and synthesis of tubulin and histone deacetylase inhibitor based on iso-combretastatin A-4, J. Med. Chem. 61 (2018) 6574–6591.
[7] C.J. Maguire, Z. Chen, V.P. Mocharla, M. Sriram, T.E. Strecker, E. Hamel, H. Zhou, R. Lopez, Y. Wang, R.P. Mason, D.J. Chaplin, M.L. Trawick, K.G. Pinney, Synthesis of dihydronaphthalene analogues inspired by combretastatin A-4 and their biological evaluation as anticancer agents, Med. Chem. Comm. 9 (2018) 1649–1662.
[8] Y. Liu, D. Yang, Z. Hong, S. Guo, M. Liu, D. Zuo, D. Ge, M. Qin, D. Sun, Synthesis and biological evaluation of 4,6-diphenyl-2-(1H-pyrrol-1-yl)nicotinonitrile analogues of crolibulin and combretastatin A-4, Eur. J. Med. Chem. 146 (2018) 185–193.
[9] Y. Pang, B. An, L. Lou, J. Zhang, J. Yan, L. Huang, X. Li, S. Yin, Design, synthesis, and biological evaluation of novel selenium-containing isocombretastatins and phenstatins as antitumor agents, J. Med. Chem. 60 (2017) 7300–7314.
[10] E.K. Jung, E. Leung, D. Barker, Synthesis and biological activity of pyrrole analogues of combretastatin A-4, Bioorg. Med. Chem .Lett. 26 (2016) 3001–3005.
[11] Q.S. Ng, H. Mandeville, V. Goh, R. Alonzi, J. Milner, D. Carnell, K. Meer, A.R. Padhani, M.I. Saunders, P.J. Hoskin, Phase Ib trial of radiotherapy in combination with combretastatin-A4-phosphate in patients with non-small-cell lung cancer, prostate adenocarcinoma, and squamous cell carcinoma of the head and neck, Ann. Oncol. 23 (2012) 231–237.
[12] M. Zweifel, G.C. Jayson, N.S. Reed, R. Osborne, B. Hassan, J. Ledermann, G. Shreeves, L. Poupard, S.P. Lu, J. Balkissoon, D.J. Chaplin, G.J.S. Rustin, Phase II trial of combretastatin A4 phosphate, carboplatin, and paclitaxel in patients with platinum-resistant ovarian cancer, Ann. Oncol. 22 (2011) 2036–2041.
[13] G.J. Rustin, G. Shreeves, P.D. Nathan, A. Gaya, T.S. Ganesan, et al., A Phase Ib trial of CA4P (combretastatin A-4 phosphate), carboplatin, and paclitaxel in patients with advanced cancer, Br. J. Canc. 102 (2010) 1355–21360.
[14] G.R. Pettit, M.R. Rhodes, D.L. Herald, E. Hamel, J.M. Schmidt, R.K. Pettit, Antineoplastic agents. 445. Synthesis and evaluation of structural modifications of (Z)- and (E)-combretastatin A-41, J. Med. Chem. 48 (2005) 4087–4099.
[15] T.F. Greene, S. Wang, L.M. Greene, S.M. Nathwani, J.K. Pollock, A.M. Malebari,

T. McCabe, B. Twamley, N.M. O'Boyle, D.M. Zisterer, M.J. Meegan, Synthesis and biochemical evaluation of 3-phenoxy-1,4-diarylazetidin-2-ones as tubulin-targeting antitumor agents, J. Med. Chem. 59 (2016) 90–113.
[16] Q. Zhang, Y. Peng, X.I. Wang, S.M. Keenan, S. Arora, W.J. Welsh, Highly potent triazole-based tubulin polymerization inhibitors, J Med Chem. 50 (2007) 749–754.
[17] S. Zheng, Q. Zhong, M. Mottamal, et al., Design, synthesis, and biological evaluation of novel pyridine-bridged analogues of combretastatin-a4 as anticancer agents, J. Med. Chem. 57 (2014) 3369–3381.
[18] K.E. Arnst, Y. Wang, D.J. Hwang, Y. Xue, et al., A potent, metabolically stable tubulin inhibitor targets the colchicine binding site and overcomes taxane resistance, Canc. Res. 78 (2018) 265–277.
[19] M. Gilandoust, K.B. Harsha, C.D. Mohan, A.R. Raquib, S. Rangappa, V. Pandey, P.E. Lobie, Basappa, K.S. Rangappa, Synthesis, characterization and cytotoxicity studies of 1,2,3-triazoles and 1,2,4-triazolo [1,5-a]pyrimidines in human breast cancer cells, Bioorg. Med. Chem. Lett. 28 (2018) 2314–2319.
[20] G. Sáez-Calvo, A. Sharma, F.A. Balaguer, I. Barasoain, Triazolopyrimidines are microtubule-stabilizing agents that bind the vinca iInhibitor site of tubulin, Cell Chem. Biol. 24 (2017) 737–750.
[21] R.Y. Qu, Y.C. Liu, W.M.W.W. Kandegama, Q. Chen, G.F. Yang, Recent applications of triazolopyrimidine-based bioactive compounds in medicinal and agrochemical chemistry, Mini. Rev. Med. Chem. 18 (2018) 781–793.
[22] Y. Luo, S. Zhang, Z.J. Liu, W. Chen, J. Fu, Q.F. Zeng, H.L. Zhu, Synthesis and antimicrobical evaluation of a novel class of 1,3,4-thiadiazole: derivatives bearing 1,2,4-triazolo[1,5-a] pyrimidine moiety, Eur. J. Med. Chem. 64 (2013) 54–61.
[23] B. Huang, C. Li, W. Chen, T. Liu, et al., Fused heterocycles bearing bridgehead nitrogen as potent HIV-1 NNRTIs. Part 3: optimization of [1,2,4]triazolo[1,5-a] pyrimidine core via structure-based and physicochemical property-driven approaches, Eur. J. Med. Chem. 92 (2015) 754–765.
[24] H. Wang, M. Lee, Z. Peng, B. Blázquez, E. Lastochkin, M. Kumarasiri, R. Bouley, M. Chang, S. Mobashery, Synthesis and evaluation of 1,2,4-triazolo[1,5-a]pyrimidines as antibacterial agents against enterococcus faecium, J. Med. Chem. 58 (2015) 4194–4203.
[25] Y.C. Liu, R.Y. Qu, Q. Chen, J.F. Yang, N. Cong-Wei, X. Zhen, G.F. Yang, Triazolopyrimidines as a new herbicidal lead for combating weed resistance associated with acetohydroxyacid synthase mutation, J. Agric. Food Chem. 64 (2016) 4845–4857.
[26] C.N. Chen, Q. Chen, Y.C. Liu, X.L. Zhu, C.W. Niu, Z. Xi, G.F. Yang, Syntheses and herbicidal activity of new triazolopyrimidine-2-sulfonamides as acetohydroxyacid synthase inhibitor, Bioorg. Med. Chem. 18 (2010) 4897–4904.
[27] C.N. Chen, L.L. Lv, F.Q. Ji, Q. Chen, H. Xu, C.W. Niu, Z. Xi, G.F. Yang, Design and synthesis of N-2,6-difluorophenyl-5-methoxyl-1,2,4-triazolo[1,5-a]-pyrimidine-2-sulfonamide as acetohydroxy acid synthase inhibitor, Bioorg. Med. Chem. 17 (2009) 3011–3017.
[28] F.Q. Ji, C.W. Niu, C.N. Chen, Q. Chen, G.F. Yang, Z. Xi, C.G. Zhan, Computational design and discovery of conformationally flexible inhibitors of acetohydroxyacid synthase to overcome drug resistance associated with the W586L mutation, ChemMedChem 3 (2008) 1203–1206.
[29] Q. Chen, X.L. Zhu, L.L. Jiang, Z.M. Liu, G.F. Yang, Synthesis, antifungal activity and CoMFA analysis of novel 1,2,4-triazolo[1,5-a]pyrimidine derivatives, Eur. J. Med. Chem. 43 (2008) 595–603.
[30] P. Chen, Y.X. Zhuang, P.C. Diao, F. Yang, S.Y. Wu, L. Lv, W.W. You, P.L. Zhao, Synthesis, biological evaluation, and molecular docking investigation of 3-amidoindoles as potent tubulin polymerization inhibitors, Eur. J. Med. Chem. 162 (2018) 525–533.
[31] P.C. Diao, Q. Li, M.J. Hu, Y.F. Ma, W.W. You, K.H. Hong, P.L. Zhao, Synthesis and biological evaluation of novel indole-pyrimidine hybrids bearing morpholine and thiomorpholine moieties, Eur. J. Med. Chem. 134 (2017) 110–118.
[32] Y.H. Li, B. Zhang, H.K. Yang, Q. Li, P.C. Diao, W.W. You, P.L. Zhao, Design, synthesis, and biological evaluation of novel alkylsulfanyl-1,2,4-triazoles as cis-restricted combretastatin A-4 analogues, Eur J Med Chem. 125 (2017) 1098–1106.
[33] B. Zhang, Y.H. Li, Y. Liu, Y.R. Chen, E.S. Pan, W.W. You, P.L. Zhao, Design, synthesis and biological evaluation of novel 1,2,4-triazolo [3,4-b][1,3,4] thiadiazines bearing furan and thiophene nucleus, Eur. J. Med. Chem. 103 (2015) 335–342.
[34] Q. Li, H.K. Yang, Q. Sun, W.W. You, P.L. Zhao, Design, synthesis and antiproliferative activity of novel substituted 2-amino-7,8-dihydropteridin-6(5H)-one derivatives, Bioorg. Med. Chem. Lett. 27 (2017) 3954–3958.
[35] F. Xie, H. Zhao, D. Li, H. Chen, H. Quan, X. Shi, L. Lou, Y. Hu, Synthesis and biological evaluation of 2,4,5-substituted pyrimidines as a new class of tubulin polymerization inhibitors, J. Med. Chem. 54 (2011) 3200–3205.
[36] Sybyl 7.3, Tripos Inc., 1699 South Hanley Road, St. Louis, MO 63144, U.S.A.
[37] R.B.G. Ravelli, B. Gigant, P.A. Curmi, I. Jourdain, S. Lachkar, A. Sobel, M. Knossow, Insight into tubulin regulation from a complex with colchicine and a stathmin-like domain, Nature 428 (2004) 198–202.
[38] W.L. DeLano, DeLano Scientific, San Carlos, CA, USA, 2002. http://www.pymol.org.